Arabian Journal of Mathematics

L. Hamolli · M. Hafizi · F. De Paolis · A. A. Nucita

Free-floating planets in the Milky Way

Abstract Gravitational microlensing is a powerful method to search for and characterize exoplanets, and it was first proposed by Paczyński in 1986. We provide a brief historical excursus of microlensing, especially focused on the discoveries of free-floating planets (FFPs) in the Milky Way. We also emphasize that, thanks to the technological developments, it will allow to estimate the physical parameters (in particular the mass and distance) of FFPs towards the center of our Galaxy, through the measure of the source finite radius, Earth or satellite parallax, and/or astrometric effects.

Mathematics Subject Classification 85-xx · 85-08

1 Introduction

Discovery of the extrasolar planets in our Galaxy is one of the most discussed issues in the scientific community. These objects are outside our solar system and have masses smaller than about $0.01 M_{\odot}$. Their detection is being achieved using different methods and, until now, we have 3824 confirmed exoplanes (see the website http://exoplanet.eu). Most exoplanets are discovered by the Transit method ($\sim 74\%$) and by Radial Velocity method ($\sim 20\%$). A few exoplanets have been detected using the Direct Imaging technique. Until now, only $\sim 2\%$ of exoplanets have been detected through gravitational microlensing.

In recent years, several unbound objects with mass possibly as small as a few times that of Jupiter ($M_J = 9.5 \times 10^{-4} M_{\odot}$) have been found in many young star-forming region using infrared imaging surveys [1]. These objects are called free-floating planets or also rogue planets, nomads, or orphan planets (see [2] and references therein). Examples of objects of this kind are WISE 0855-0714, about 2.4 pc away from the Earth [3], and Cha 110913–773444 in the Chamaeleon I star-forming region at a distance of about 160 pc. It is difficult to find this kind of objects by infrared imaging at large distances, so we need the development of alternative methods to search for them. The origin of the FFPs is doubtful, and their formation mechanism remains an open theoretical question in astrophysics. One possibility is that they originally formed around a host star and then scattered out from orbit. A second option is that they may form on their own through gas cloud direct collapse, similarly to star formation.

L. Hamolli · M. Hafizi
Department of Physics, University of Tirana, Tirana, Albania

F. De Paolis (✉) · A. A. Nucita
Department of Mathematics and Physics "Ennio De Giorgi", University of Salento, 73100 Lecce, Italy
E-mail: francesco.depaolis@unisalento.it

F. De Paolis · A. A. Nucita
INFN, Sezione di Lecce, CP 193, 73100 Lecce, Italy

🖉 Springer

Paczyński [4] first envisaged the search of Galactic dark matter in compact form using gravitational lensing method, which happens when a massive object passes close enough to the line of sight to a distant source star. Since the angular separation of the lensed images are of the order of microarcseconds, such phenomena are often called microlensing [5,6]. In his calculations, Paczyński showed that the chance (or optical depth) of a massive object in the Galactic halo to serve as a lens and magnify a background star in nearby galaxy is $\simeq 10^{-6}$. Also, he suggested that, based on modern instruments, we could be able to catch such microlensing events by monitoring a dense stellar field with several millions of stars simultaneously. Therefore, several ground-based experiments such as MACHO (Massive astrophysical compact halo object) [7], EROS (Experience pour la Recherche d'Objets Sombres) [8], OGLE (Optical Gravitational Lensing Experiment) [9], and MOA (Microlensing Observations in Astrophysics) [10] were carried out, aiming at the closest dense stellar fields as Magellanic Clouds and Galactic bulge. The first microlensing events were announced by the MACHO team [11].

Since the gravitational microlensing phenomenon does not rely on the flux output from the lensing object, it is the only method for detection of dark objects, as FFPs. It is also worth noting that, recently, a population of FFPs in a far-away galaxy has been probed using the Quasar microlensing technique in the X-ray band [12]. Microlensing events caused by FFPs are rather short in time (of the order of a few days), so ground-based observations may detect them only with great difficulties, so to search for lens masses below about $0.01 M_\odot$, as for FFPs, space-based observations are expected to give much better results. Untill now such surveys are performed by Kepler and Spitzer telescopes. The Kepler observatory, which is moving in an Earth-trailing Solar orbit, had the primary mission aim to explore exoplanet demographics using the transit method. The mechanical failure of the second of its four reaction wheels in 2013 signaled the conclusion of the primary mission, but heralded the genesis of an extended K2 Mission. It performed the microlensing survey towards the Galactic bulge from April 7 to July 1, 2016 called K2C9 (see [13] and references therein). K2C9 lasted for about 3 months and this observational period overlapped with that of the Spitzer follow-up microlensing project that started in June, 2016. Spitzer was the first satellite employed to conduct real-time monitoring of a microlensing event simultaneously with ground-based facilities [14]. During its program, the satellite parallax microlensing for an isolated star [15] and a planetary system [16] are measured. Two additional Spitzer programs developed during 2016: the first one to explore the Galactic distribution of exoplanets using high-magnification microlensing events and the other to conduct a two satellite microlensing experiment [17] by observing in conjunction with K2C9. At present, there are two space-based missions which are planned for detecting microlensing events towards the Galactic bulge: the Wide-Field Infrared Survey Telescope (WFIRST) [18] and Euclid [19], although the last news from Euclid seem to indicate that the microlensing program will not be actually performed. Based on the capabilities of their facilities, we have foreseen the detection of the FFP population in our Galaxy [20].

Besides photometric observations, a microlensing event can be detected also astrometrically. The best instrument for such observations is the Gaia satellite. Gaia is a space observatory of the European Space Agency (ESA) launched on 19 December 2013, and is performing the astrometric, photometric, and spectroscopic observations for more than 1 billion stars in our Milky Way and neighboring galaxies. While Gaia satellite is observing the full sky, follow-up astrometric surveys of the interesting microlensing events are planned to be obtained by ground-based instruments as GRAVITY, which is a Very Large Telescope Interferometer build by the European Southern Observatory and the Max Planck Institute for Extraterrestrial Physics [21,22].

The first attempts to characterize the FFP population in our Galaxy have been conducted by Sumi et al. [23]. They analyzed the light curves of 474 microlensing events observed during a 2-year survey by the MOA-II collaboration towards the Galactic bulge and by analyzing their timescale distribution, which reported the discovery of planetary-mass objects either very distant from their host star (i.e., orbiting at distances larger than 100 AU) or fully unbound. It was found an excess of short-timescale events, with duration below 2 days, with respect to the expectations based on the extrapolation of the stellar mass function down to low-mass Brown Dwarfs (BDs). A best-fit procedure to the observed microlensing events due to FFPs in the mass range, 10^{-5}–$10^{-2} M_\odot$, has also allowed to extend and constrain the power-law mass function at the low-mass regime of the FFPs with the index $\alpha_{PL} = 1.3^{+0.3}_{-0.4}$ and to determine the number N_{PL} of planetary-mass objects per star to be: $N_{PL} = 5.5^{+18.1}_{-4.3}$. The poor precision of the N_{PL} value is mainly due to the large uncertainty of the lens mass estimate below $10^{-4} M_\odot$.

Later on, the simulations conducted by Veras and Raymond [24] and Pfyffer et al. [25] for the formation and evolution of planetary systems asserted that planet–planet scattering itself is insufficient to produce the abundance of FFP candidates seen by MOA-II. In any case, Silk [26] found that opacity limited fragmentation of collapsing clouds could produce a fragment with a minimum mass as low as $\sim 0.01 M_\odot$. Moreover, turbulent

shock could cause them to become gravitationally unstable and collapse into objects with the mass of giant planets [27], thus implying the possible presence of a large number of FFPs in galaxies. Recently, Mróz et al. [28] reported on the analysis of a large sample of microlensing events discovered during the years $2010 \div 2015$ by OGLE collaboration. They found no excess of events with timescales smaller than 2 days, but detected a few possible ultrashort-timescale events (with timescales of less than 0.5 day), which may indicate the existence of Earth-mass and super-Earth-mass FFPs. Therefore, knowing the FFP population in our Galaxy is still an open question and the gravitational microlensing is the only method capable of exploring the entire population of FFPs down to Mars-mass objects.

Based on the results obtained by Sumi et al. [23] and the capabilities of different telescopes, which are performing microlensing observations and/or are planned for the near future, we have considered the issue of the FFP detection by gravitational microlensing in the Milky Way. We estimate the detection efficiency (that is ratio between the number of events for which each second-order effect is detectable and the number of simulated events) of the finite source effect, orbital or satellite parallax and astrometric effect in microlensing events caused by FFPs towards the Galactic bulge. These effects are very important for the determination of the FFP physical parameters (mass and distance) due to the microlensing degeneracy. Here, we also note that microlensing events toward the Galactic bulge can be caused by different object such as stars, BD, and FFPs, which are in the field of view of the telescope. For these objects, we have considered the following density distributions: (a) exponential thin and thick disk and (b) triaxial bulge [29]. In addition, for the their velocity distribution, we have assumed a Maxwellian distribution [30,31]. Based on Sumi et al. [23], the FFP and BD mass functions are considered as power law with indexes: $\alpha_{\mathrm{PL}} = 1.3^{+0.3}_{-0.4}$ and $\alpha_{\mathrm{BD}} = 0.49^{+0.24}_{-0.27}$, respectively. The abrupt change from $\alpha_{\mathrm{PL}} \simeq 1.3$ to $\alpha_{\mathrm{BD}} \simeq 0.49$ favors the idea of two separate populations, as if the FFP formation process is different from that of stars and BDs. The optical depth and the microlensing rate of events caused by FFPs were calculated in Ref. [20] where it was found that these events are much fewer with respect to those due to main sequence stars, but more numerous than those due to BDs. Considering the lower limit of the FFPs per star, we found that by space-based telescopes (in particular by Euclid or WFIRST) will be detected about 100 microlensing events caused by FFPs during a month (see Ref. [20] for details). Moreover, since the FFPs are not expected to be surrounded by a plasma, we have not considered its effect in the gravitational microlensing events [32]. However, whether a microlensing event is caused by a primordial black hole, modeling the plasma-induced effects on the light curve is compelling (see [33]). In the next sections, we review the bases of microlensing and in particular on the photometric aspects. Then, in Sect. 3, we discuss astrometric microlensing and, in Sect. 4, we show how to break the degeneracy in microlensing events caused by FFPs. Our conclusions are presented in Sect. 5.

2 Basics of photometric microlensing

Gravitational microlensing method is a well-known technique for detecting compact objects in the disk, bulge, and/or halo of our Galaxy via the time-dependent amplification of the light from background sources. In the simplest case, when the point-like approximation for both lens and source is assumed, and the relative motion among the observer, lens, and source is uniform and linear, individual images cannot be resolved due to their small separation, but the total brightness of the images is larger with respect to that of the unlensed source, leading to a specific time-dependent amplification of the source [4,34]. For a source at angular distance θ_{S} from a point-like gravitational lens with mass M, the positions θ of the two images with respect to the lens are obtained by solving the lens equation (see Ref. [35]):
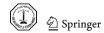
$$\tilde{u}^2 - u\tilde{u} - 1 = 0, \tag{1}$$

where $u = \theta_{\mathrm{S}}/\theta_{\mathrm{E}}$ and $\tilde{u} = \theta/\theta_{\mathrm{E}}$ are the dimensionless distances and θ_{E} is the Einstein angular radius. When the observer, the lens, and the source are perfectly aligned, the source image becomes a ring, called the Einstein ring. The angular Einstein ring radius can be expressed as follows:

$$\theta_{\mathrm{E}} = \sqrt{\frac{4GMD_{\mathrm{S}}}{c^2}\frac{D_{\mathrm{S}} - D_{\mathrm{L}}}{D_{\mathrm{L}}D_{\mathrm{S}}}} \simeq 2851\mu as\sqrt{\frac{M(M_\odot)}{D_{\mathrm{L}}(\mathrm{kpc})}\left[1 - \frac{D_{\mathrm{L}}(\mathrm{kpc})}{D_{\mathrm{S}}(\mathrm{kpc})}\right]}. \tag{2}$$

Here, D_{S} and D_{L} are the distances to the source and the lens, respectively. The solutions of Eq. (1) are as follows:

$$\tilde{u}_{+,-} = \frac{1}{2}(u \pm \sqrt{4 + u^2}), \tag{3}$$

which give the locations of the positive and negative parity images ($+$ and $-$, respectively) with respect to the lens position. Note that, in the lens plane, the $+$ image resides always outside the Einstein ring centered on the lens position, while the $-$ image is always within this ring. Due to the conservation of the surface brightness, the amplification of the background source is simply given by the ratio between the area of the images to the area of the source. Therefore, the time-dependent amplification of the distorted images can be calculated by the following:

$$A = |A_+| + |A_-| = \frac{2 + u^2}{u\sqrt{4 + u^2}} \geq 1. \tag{4}$$

If we assume the relative lens–source motion to be rectilinear, u can be decomposed into the components parallel and perpendicular to the direction of the relative lens source motion. Thus, $u(t)$ and $A(t)$ can be calculated as follows:

$$u(t) = \sqrt{\left(\frac{t - t_0}{t_E}\right)^2 + u_0^2}, \ A(t) = \frac{2 + u(t)^2}{u(t)\sqrt{4 + u(t)^2}}, \tag{5}$$

where t_0 and u_0 are the time and impact parameter at the closest approach. Here, t_E is the Einstein timescale, which is defined as the time required for the lens to transit the Einstein radius:

$$t_E = \frac{\theta_E}{\mu_{rel}} = \frac{R_E}{v_T}, \tag{6}$$

where μ_{rel} is the relative lens–source velocity, R_E is Einstein radius ($R_E = \theta_E D_L$), and v_T is the lens–source–observer relative transverse velocity.

During a microlensing event, the source position projected in the lens plane encounters the Einstein ring when the projected separation is $u = 1$, where the source amplification takes the value $A_{th} = 1.34$ called the threshold amplification. For space-based observations, due to the absence of seeing effects, the amplification threshold may be much smaller than 1.34, with a corresponding much larger value for the parameter u. Assuming a photometric error $\sim 0.1\%$, the threshold amplification turns out to be $A_{th} = 1.001$ and the maximum value of u from Eq. (5) turns out to be $u_{max} = 6.54$ [20].

One has to consider at this point that, from the event lightcurve, three parameters can be defined: the time of maximum amplification t_0, the Einstein time t_E, and the impact parameter u_0. However, of these parameters, only t_E contains information about the lens and this gives rise to the so-called parameter degeneracy problem, since there are only two observable quantities. This degeneracy cannot allow to infer the lens parameters uniquely, thus making the interpretation of microlensing results somewhat ambiguous. To break this degeneracy, we consider the second-order effects, which are the finite source effects (see Refs. [36–39]) and the parallax effect. In principle, there are two ways to observe the shift caused by the parallax effect. First, the orbital motion of the Earth (annual parallax) creates on the light curve a shift relative to the simple straight motion between the source and lens (see Refs. [40,43,44]). Second, two observers at different locations looking contemporarily towards the same event can compare their observations [14]. These second-order effects induce small deviations in the light curve (with respect to the Paczyński profile), which may be extremely useful to break, at least partially, the parameter degeneracy problem in microlensing observations.

3 Basics of astrometric microlensing

It is well known that, in addition to the photometric lightcurve, a gravitational microlensing event gives rise also to an astrometric deflection, as the event unfolds. This is because the images produced by the lens are not symmetrically distributed, leading to a typical elliptic pattern traced by the centroid, which was studied by many authors [45–49]. The centroid of the image pair can be defined as the average position of the $+$ and $-$ images weighted by the associated magnifications [50,51]:

$$\bar{u} = \frac{\tilde{u}_+ A_+ + \tilde{u}_- A_-}{A_+ + A_-} = \frac{u(u^2 + 3)}{u^2 + 2}, \tag{7}$$

so that, by symmetry, the image centroid is always aligned with the lens and the source. The measurable quantity is the displacement Δ of the centroid of the image pair relative to the source, that is:

$$\Delta = \bar{u} - u = \frac{u}{u^2 + 2}, \tag{8}$$

which, of course is a function of time, since u depends on time. While the image magnification, A is a dimensionless quantity which depends only on the dimensionless separation u, and Δ is a function of both u and the angular Einstein ring radius θ_E, so that the observed centroid shift is directly proportional to θ_E:

$$\Delta = \frac{u}{u^2 + 2} \theta_E. \tag{9}$$

It is straightforward to show that during a microlensing event of a single lens on a single source, the centroid shift, Δ, traces an ellipse. The ellipse semi-axes a and b, which depend on both the lens impact parameter u_0 and θ_E, are given by the following:

$$a = \frac{1}{2} \frac{\theta_E}{\sqrt{u_0^2 + 2}}, \quad b = \frac{1}{2} \frac{u_0}{u_0^2 + 2} \theta_E. \tag{10}$$

The Einstein angular radius in microlensing events caused by FFPs is typically of the order of a few μas. For this reason, the astrometric signal is expected to be detected more efficiently through space-based observations, as those by the Gaia satellite. Its precision for astrometric observations depends on the visual magnitude of the star. Eric Hog [52] has determined the astrometric precision of the Gaia telescope and found that it can be as low as 4 μas for stars with visual magnitude in range from 6 to 13 (see table A in Ref. [52]).

4 Solving the parameter degeneracy

As mentioned above, from the parameters obtained by the light curve of a microlensing event, only t_E contains information about the lens. Therefore, to infer the lens properties uniquely, we have considered the second-order effects, from which the microlens parallax π_E and the angular Einstein radius θ_E can be determined. Gould [53] pointed out that the microlens parallax is given by the following:

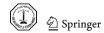$$\pi_E = \frac{AU}{r_E}, \tag{11}$$

where r_E is the Einstein radius projected on the observer plane. If r_E is measured, then the mass of the lens can be determined without ambiguity by the following:

$$M = \frac{\theta_E}{\kappa \pi_E}, \tag{12}$$

where $\kappa \equiv \frac{4G}{c^2 AU} = 8.144 \frac{mas}{M_\odot}$. The microlens parallax can be derived from the orbital parallax, which is caused by the orbital motion of the observer (Earth) around the Sun [54] and by the simultaneous observation of the source microlensing event by two telescopes at different locations. Indeed, during a microlensing event, the deviations of the light curve from the symmetrical shape, due to the Earth orbital motion, can be observed [40–42]. The information of microlens parallax can be obtained by modeling and fitting the tiny asymmetry in the light curve. In addition, the microlens parallax can be detected by analyzing the photometric curves detected by two telescopes that are far away from each other [14]. The value of the angular Einstein radius can be obtained by measuring finite source effects, from high-resolution imaging and from astrometric measurements. More detailed descriptions of each method are provided in the following sections.

Before closing this section, we note that in our numerical simulations, we have assumed that a microlensing event can be detected if, in its light curve, there are at least 8 points in which the amplification is bigger than the threshold amplification. For space-based observations, the threshold amplification is assumed $A_{th} = 1.001$. The parallax effect and finite source effects can be detected on a light curve when the residuals with respect to the Paczyński curve are larger than 0.001.
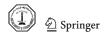
4.1 π_E in microlensing events caused by FFPs

The parallax effect, due to the motion of the Earth around the Sun, may leave in the light curve of microlensing events observable features, which can be used to constrain the lens parameter. Alcock et al. [40] have presented the first detection of parallax effects in a gravitational microlensing event. Their description of the parallax effect in the light curves was obtained by expanding the Earth trajectory up to the first order in the eccentricity. For relatively long events (with duration about a few months), the deviations by the Earth motion may be consistent, and so, one can determine microlens parallax, π_E. However, in the case of space observatories (like WFIRST or Euclid positioned at the $L2$ point), the satellite acceleration around the Sun can produce a parallax effect that can be detectable also for short-duration microlensing events as those caused by FFPs [20]. Following the analysis by Dominik [43] and based on the capabilities of space telescopes, we found that nearly 30% of the events caused by FFPs towards the Galactic bulge may have detectable orbital parallax effect. We also found that the best period during the year to observe the parallax effect is June, due to the orientation of the Earth orbital plane with respect to the line of sight towards the bulge [44].

Another way to estimate the microlens parallax can be provided using two telescopes: one located on the Earth and the other one in space, provided that they observe the same event contemporarily. The possibility to measure the microlens parallax through the simultaneous observations of the same microlensing event by two telescopes distant enough from each other has been set by Refsdal [6] and later developed by Gould [55]. The era of space-based microlensing parallax observations started much later using Spitzer with the analysis of an SMC event [14] and, later on, continued with the ongoing Spitzer observational campaign started in 2014 for the follow-up of the microlensing events detected towards the Galactic bulge [56–59]. This observational campaign has already led to several important results assessing clearly the importance of these kinds of measurements. By the two photometric curves, the shift time at the peak $\Delta t_0 = \mid t_{0,\oplus} - t_{0,\text{sat}} \mid$ and $\Delta u_0 = \mid u_{0,\oplus} - u_{0,\text{sat}} \mid$ can be measured, and consequently, $\pi_E = \frac{\text{AU}\Delta u}{D_\perp}$ can be estimated, being $\Delta u = (\frac{\Delta t_0}{t_E}, \Delta u_0)$ and $D_\perp$ the projected separation between the two telescopes in the observer plane. Since $D_\perp$ is known, one can determine the microlens parallax. In the case of large values of $D_\perp$, the light curves seen from two observers will exhibit noticeable difference in the parallax effect (see Ref. [13] for details). Considering the photometric observations towards the Galactic bulge, by the Earth (OGLE) and the space telescopes (K2C9 and Spitzer), we calculated the probability that a microlensing event is detected by two telescopes simultaneously. This probability depends on the mass function index α_{PL} and the space distribution of the FFPs. It is larger at the beginning of the compaign, while it decreases towards the end of it. The detection probability of a microlensing event by OGLE–K2 pair of the telescopes is bigger than by OGLE–Spitzer pair. Moreover, it depends on their threshold amplification and their projected separation.

4.2 θ_E in microlensing event caused by FFPs

As already anticipated in section 1, the angular Einstein radius can be obtained when finite source effects in the microlensing light curve are detectable. In these events, the value of u_0 becomes comparable to the source radius projected onto the lens plane in units of the Einstein radius and the resulting light curve deviates from the standard form of a point-source event [60]. These deviations depend on the light intensity distribution throughout the source stellar disk. Different brightness profiles have been proposed and discussed in the literature. Among them, that describing the light intensity distribution in the stellar disk more accurately than any other model is the non-linear limb-darkening model [61]. By fitting the microlensing light curve with the Claret model for the source's disk limb-darkening profile, one can define the source radius projected onto the lens plane in units of the Einstein radius. If the angular size of the source may be estimated through the color and the absolute magnitude of the source, then the angular Einstein radius can be measured. For example, Zub et al. [62] have presented a detailed analysis of the highly sampled OGLE 2004-BLG-482 event and have determined the source star limb-darkening coefficients (LDCs) and the angular Einstein radius, which results to be $\simeq 0.4\ \mu as$. Using the LCDs given by the Claret model, we found that the probability of the finite source effect in microlensing events caused by FFPs is about 30% [39].

In the case of bright lens (when the lens is a star), the angular Einstein radius can be detected by the high-resolution imaging. Long after the microlensing event, by taking a snapshot with very high precision astrometry, one can easily calculate the relative lens–source velocity μ_{rel}. Combined with the Einstein timescale t_E obtained from the light curve, one can thus derive the Einstein radius [63]. In our calculation, we have not considered this method, because the FFPs are not bright objects.

Table 1 Efficiency of some second-order effects in microlensing events caused by FFPs towards the Galactic bulge as a function of the α_{PL} value in the range 0.9–1.6 and for observing cadence of 20 min and 30 min

α_{PL}	Cadence 20 min		Cadence 30 min		
	Finite source efficiency	Orbital parallax efficiency	Satellite paralax efficiency (E–K2C9)	Satellite paralax efficiency (E–S)	Astrometric efficiency
0.9	0.220	0.330	0.915	0.462	0.166
1.0	0.250	0.328	0.890	0.424	0.099
1.1	0.269	0.321	0.858	0.349	0.076
1.2	0.294	0.314	0.814	0.299	0.070
1.3	0.318	0.312	0.774	0.249	0.064
1.4	0.336	0.304	0.739	0.207	0.053
1.5	0.359	0.302	0.701	0.158	0.041
1.6	0.371	0.229	0.672	0.130	0.036

Another way to determine the Einstein radius is through astrometric microlensing. The most extensive work on astrometric microlensing was provided by Dominik and Sahu [47], who provided a thorough review of astrometric microlensing of stars. The idea of astrometric microlensing is that, although the state-of-art observatories are not able to resolve the two microlensed images, it is possible to measure the astrometric shift of the centroid of the two images with respect to the source star position. If we consider a source star in the bulge of our Galaxy ($D_S = 8.5$ kpc) and the lens (FFP with mass in the range $[10^{-5}, 10^{-2}]M_\odot$) in the middle of the observer–source distance, the Einstein angular radius results to be, from Eq. (2) in the range $3 \div 98 \, \mu as$. Since, for microlensing events with $u_0 \leq \sqrt{2}$, the maximum value of the centroid shift is given by $\Delta_{\max} \simeq 0.35 \, \theta_E$, it results in the range $1 \div 35 \, \mu as$. These events are astrometrically detectable if the precision of the astrometric observation is good enough. In Ref. [64], the astrometric signal in microlensing events caused by FFPs by the Gaia space telescope is discussed. These measurements, in combination with photometric observations, can be used to precisely constrain the FFP mass.

Of course, the efficiency of the astrometric effect (that is, in other words, the percentage of events with detectable astrometric shift) depends on the value of the FFP mass function index and it decreases when the value of D_L is increased (see [64] for details). In Table 1, we give the efficiency values of the second-order effects in microlensing events caused by the FFPs towards Galactic bulge. Here, the FFPs are considered to be distributed in the thin Galactic disk and the values of the α_{PL} are in the range 0.9–1.6. As one can see, the finite source efficiency is increased with α_{PL}, while the efficiency of the orbital parallax, satellite parallax (for the pairs: Earth–K2C9 and Earth–Spitzer) and astrometric shift decreases with increasing α_{PL} (see Refs. [13,20,39,64] for details).
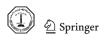
5 Conclusions

In this paper, we have discussed and stressed that the gravitational microlensing method is the best one to obtain valuable information about the population of FFPs in the Milky Way. Both photometric and astrometric microlensing observations are very important to solve the parameter degeneracy, at least in a sub-sample of the observed events, and determine the lens parameters. We have stressed that space-based observations are particular important not only to the number of detected microlensing events caused by FFPs, but also for the detection of the second-order effects such as finite source, parallax, and astrometric effects. The first two effects may be detected in surveys as those conducted by Kepler and Spitzer telescopes or by future missions as WFIRST and Euclid, while the latter effect is within the objectives of the Gaia mission.

References

1. Zapatero Osorio, M.R.; et al.: Discovery of young, isolated planetary mass objects in the orionis star cluster. Science **290**, 103 (2000)
2. Strigari, L.E.; et al.: Nomads of the galaxy. MNRAS **1856**, 423 (2012)
3. Luhman, K.L.; Esplin, T.L.: A new parallax measurement for the coldest known Brown Dwarf. Astrophys. J. **796**, 6 (2014)
4. Paczyński, B.: Gravitational microlensing by the galactic halo. Astrophys. J. **304**, 1 (1986)
5. Liebes, S.: Gravitational lenses. Phys. Rev. **133**, 835 (1964)
6. Refsdal, S.: The gravitational lens effect. MNRAS **128**, 295 (1964)
7. Alcock, C.; Allsman, R.A.; Axelrod, T.S.; et al.: The MACHO Project—a search for the dark matter in the Milky-Way. ASPC **43**, 291 (1993)
8. Aubourg, E.; Bareyre, P.; Brehin, S.; et al.: The EROS search for dark halo objects. Messenger **72**, 20 (1993)
9. Udalski, A.; Szymanski, M.; Kaluzny, J.; et al.: The optical gravitational lensing experiment. Acta Astron. **42**, 253 (1992)
10. Muraki, Y.; Sumi, T.; Abe, F.; et al.: Search for Machos by the MOA collaboration. Prog. Theor. Phys. Suppl. **133**, 233 (1999)
11. Alcock, C.; Akerlof, C.W.; Allsman, R.A.; et al.: Possible gravitational microlensing of a star in the large magellanic cloud. Nature **365**, 621 (1993)
12. Dai, X.; Guerras, E.: Probing extragalactic planets using quasar microlensing. Astrophys. J. **853**, 27 (2018)
13. Hamolli, L.; De Paolis, F.; Hafizi, M.; Nucita, A.A.: Predictions on the detection of the free-floating planet population with K2 and spitzer microlensing campaigns. Astrophys. Bull. **72**, 73 (2017)
14. Dong, S.; Udalski, A.; Gould, A.; et al.: First space-based microlens parallax measurement: spitzer observations of OGLE-2005-SMC-001. Astrophys. J. **664**, 862 (2007)
15. Yee, J.C.; Udalski, A.; Calchi Novati, S.; et al.: First space-based microlens parallax measurement of an isolated star: spitzer observations of OGLE-2014-BLG-0939. Astrophys. J. **802**, 76 (2017)
16. Udalski, A.; Yee, J.C.; Gould, A.; et al.: Spitzer as a Microlens Parallax Satellite: mass measurement for the OGLE-2014-BLG-0124L planet and its host star. Astrophys. J. **799**, 236 (2015)
17. Henderson, C.B.; Poleski, R.; Penny, M.; et al.: Campaign 9 of the K2 Mission: observational parameters, scientific drivers, and community involvement for a simultaneous space- and ground-based microlensing survey. PASP. 128l4401H (2016)
18. Spergel, D.; et al.: Wide-field infrared survey telescope-astrophysics focused telescope assets WFIRST-AFTA 2015 report (2015). arXiv:1503.03757
19. Laureijs, R.; et al.: Euclid mission status. SPIE. 9143 E..0HL (2014)
20. Hamolli, L.; Hafizi, M.; Nucita, A.A.: A theoretical calculation of microlensing signatures caused by free-floating planets towards the galactic bulge. IJMPD **22**, 1350072 (2013)
21. Eisenhauer, F.; et al.: GRAVITY: microarcsecond astrometry and deep interferometric imaging with the VLT. ASSP **9**, 361 (2009)
22. Zurlo, A.; et al.: Performance of the VLT planet finder SPHERE. I. Photometry and astrometry precision with IRDIS and IFS in laboratory. Astron. Astrophys. **572**, 85 (2014)
23. Sumi, T.; et al.: Unbound or distant planetary mass population detected by gravitational microlensing. Nature **473**, 349 (2011)
24. Veras, D.; Raymond, S.N.: Planet–planet scattering alone cannot explain the free-floating planet population. MNRAS **421L**, 117V (2012)
25. Pfyffer, S.; Alibert, Y.; Benz, W.; Swoboda, D.: Theoretical models of planetary system formation. II. Post-formation evolution. Astron. Astrophys. **579A**, 37 (2015)
26. Silk, J.: Structure formation. ASIC **502**, 111 (1997)
27. Padoan, P.; Nordlund, Å.: The, "Mysterious" origin of brown dwarfs. APJ **617**, 559 (2004)
28. Mróz, P.; et al.: No large population of unbound or wide-orbit Jupiter-mass planets. Nature **548**, 183 (2017)
29. Hafizi, M.; De Paolis, F.; Ingrosso, G.; Nucita, A.A.: Microlensing signature of a white dwarf population in the galactic halo. IJMPDD **13**, 1831 (2004)
30. Han, C.; Gould, A.: The mass spectrum of MACHOs from parallax measurements. Astrophys. J. **447**, 53 (1995)
31. Han, C.; Gould, A.: Statistical determination of the MACHO mass spectrum. Astrophys. J. **467**, 540 (1995)
32. Morozova, V.S.; Ahmedov, B.J.; Tursunov, A.A.: Gravitational lensing by a rotating massive object in a plasma. APSS **346**, 513 (2013)
33. Abdujabbarov, A.; Toshmatov, B.; Schee, J.; et al.: Gravitational lensing by regular black holes surrounded by plasma. IJMPD. 2641011A (2017)
34. Paczyński, B.: Gravitational microlensing in the local group. ARAA **34**, 419 (1996)
35. Schneider, P.; Ehlers, J.; Falco, E.E.: Gravitational Lenses. Springer, New York (1992)
36. Nemiroff, R.J.; Wickramasinghe, W.A.D.T.: Finite source sizes and the information content of macho-type lens search light curves. APJ **424**, 21 (1994)
37. Witt, H.J.; Mao, S.: Can lensed stars be regarded as pointlike for microlensing by MACHOs? APJ **430**, 505 (1994)
38. Witt, H.J.: The effect of the stellar size on microlensing at the baade window. APJ **449**, 42 (1995)
39. Hamolli, L. Hafizi, M.; De Paolis, F.; Nucita, A.A.: Estimating finite source effects in microlensing events due to free-floating planets with the euclid survey. Adv. Astron. (2015) (**ID 402303**)
40. Alcock, C.; et al.: First observation of parallax in a gravitational microlensing event. APJ. **454**, 125 (1995)
41. Smith, M.C.; Mao, S.; Paczyński, B.: Acceleration and parallax effects in gravitational microlensing. MNRAS **339**, 925 (2003)
42. Park, B.-G.; DePoy, D.L.; Gaudi, B.S.; et al.: MOA 2003-BLG-37: a bulge jerk-parallax microlens degeneracy. APJ **609**, 166 (2004)
43. Dominik, M.: Galactic microlensing with rotating binaries. Astron. Astrophys. **329**, 361 (1998)
44. Hamolli, L.; Hafizi, M.; De Paolis, F.; Nucita, A.A.: Paralax effects on microlensing events caused by free-floating planets. Bulg. Astron. J. **19**, 34 (2013)
45. Walker, M.A.: Microlensed image motions. APJ **453**, 37 (1995)

46. Miyamoto, M.; Yoshii, Y.: Astrometry for determining the MACHO mass and trajectory. Astron. J. **110**, 1427 (1995)
47. Dominik, M.; Sahu, K.C.: Astrometric microlensing of stars. APJ **534**, 213 (2000)
48. Hog, E.; Novikov, I.D.; Polnarev, A.G.: MACHO photometry and astrometry. Astron. Astrophys. **294**, L287 (1995)
49. Nucita, A.A.; et al.: Astrometric microlensing. IJMPD. 2641015N (2017)
50. Boden, A.F.; Shao, M.; Van Buren, D.: Astrometric observation of MACHO gravitational microlensing. APJ **502**, 538 (1998)
51. Nucita, A.A.; et al.: Parallax and orbital effects in astrometric microlensing with binary sources. APJ **823**, 120 (2016)
52. Hog, E.: Astrometric accuracy during the past 2000 years. (2017). arXiv:1707.01020
53. Gould, A.A.: Natural formalism for microlensing. APJ **542**, 785 (2000)
54. Gould, A.A.: Resolution of the MACHO-LMC-5 Puzzle: the jerk-parallax microlens degeneracy. APJ **606**, 319 (2004)
55. Gould, A.: MACHO velocities from satellite-based parallaxes. APJ **421**, L75 (1994)
56. Gould, A.; Carey, S.; Yee, J.: Spitzer proposal (2013) (**ID 10036**)
57. Gould, A.; Carey, S.; Yee, J.: Spitzer proposal (2014) (**ID 11006**)
58. Gould, A.; Yee, J.; Carey, S.: Spitzer proposal (2015) (**ID 12015**)
59. Gould, A.; Yee, J.; Carey, S.: Spitzer proposal (2015) (**ID 12013**)
60. Han, C.; et al.: Gravitational microlensing: a tool for detecting and characterizing free-floating planets. APJ **604**, 372 (2004)
61. Claret, A.: A new non-linear limb-darkening law for LTE stellar atmosphere models. Calculations for $-5.0 <= \log[M/H] <= +1$, $2000\,K <= Teff <= 50000\,K$ at several surface gravities. Astron. Astrophys. **363**, 1081 (2000)
62. Zub, M.; et al.: Limb-darkening measurements for a cool red giant in microlensing event OGLE 2004-BLG-482. Astron. Astrophys. **525**, 15 (2011)
63. Kozlowski, S.; Wozniak, P.R.; Mao, S.; et al.: The first direct detection of a gravitational-lens toward the galactic bulge. APJ **671**, 420 (2007)
64. Hamolli, L.; et al.: The astrometric signal of microlensing events caused by free floating planets. APSS **363**, 153 (2018)